Plasma Production in a Small High Field Force-Balanced Coil Tokamak Based on Virial Theorem

H. Tsutsui, T. Ito, H. Ajikawa, T. Enokida, K. Hayakawa, S. Nomura, S. Tsuji-Iio, and R. Shimada, *Research Laboratory for Nuclear Reactors, Tokyo Institute of Technology*

***Abstract*— The plasma production and confinement experiments in a novel tokamak device with a new type of toroidal field (TF) coils and a central solenoid (CS) whose stress is reduced to a theoretical limit determined by the virial theorem are presented. According to the virial theorem, the best TF coil to produce the strongest magnetic field under the weakest stress requires equal averaged principal stresses in all directions. Therefore, the pitch number of a helical coil is determined to satisfy the uniform stress condition. Moreover, the helical winding is modulated in such a way that poloidal field exists only outside of a torus, because the poloidal field in the torus prevents the breakdown of plasma and causes the torsional force. In the case of the aspect ratio $A = 2$, our optimal coil theoretically increases the magnetic field to 1.4 times larger than the conventional TF coil. In order to prove the advantage of the VLC concept, we manufactured a small VLC pulsed tokamak "Todoroki-II" with a major radius of 0.3 m, a minor radius of 0.08 m, toroidal magnetic field strengths of $B_{\rm T} < 1.5$ T and plasma currents of $I_{\rm P} < 40$ kA. External vertical field increased both the plasma pulse length and current to 1 ms and 11 kA, respectively, while they were restricted because of no vertical field control. Using a Cauchy-condition surface (CCS) method, the shape and displacement of plasma boundary was reconstructed, and the validity of CCS under large eddy currents was verified.**

I. Introduction

RECENTLY we had developed a tokamak with force-balanced coils (FBCs) [1] which are multi-pole helical hybrid coils combining toroidal field (TF) coils and a central solenoid (CS). The combination reduces the net electromagnetic force in the direction of major radius [2], [3] by canceling the centering force due to the TF coil current and the hoop force due to the CS coil current. This excellent feature of FBC and its capability of tokamak reactor were investigated [1], [4] and demonstrated by the first FBC tokamak "Todoroki-I" [5], [6], while three problems came up as follows: 1) Working stress in coils has not yet been investigated while the net electromagnetic force is reduced. 2) Since stray magnetic fields due to the helical winding prevent plasma breakdown, an auxiliary coil set to cancel the vertical field and an electrode for ionization were required during plasma discharge. 3) Expected values of some parameters were not achieved owing to poor plasma control due to error field by FBC.

In this work, we extend the concepts of FBC by use of a virial theorem [7] in the next section. In section III, design of a small tokamak based on the virial theorem is explained. Operations and discharges are investigated in section IV. In section V, plasma current and surface are estimated by CCS method [8], and summarized this work in section VI.

II. Virial theorem

First of all, we have extended the FBC concept using the virial theorem [7], [9],

$$\int_\Omega \sum_i \sigma_i {\rm d}V = \int \frac{B^2}{2\mu_0} {\rm d}V = U_{\rm M}, \tag{1}$$

where $\sigma_i (i = 1, 2, 3)$ are the principal stresses in supporting structures Ω, and $U_{\rm M}$ is magnetic energy. This theorem shows that strength of magnetic field B is restricted by working stress in the coils and their supporting structure. High-field coils, which are required to achieve strong magnetic field with small stress, should accordingly have uniform distribution of principal stresses in all directions. Next we introduce a normalized stress $\tilde{\sigma}$ [9] defined by

$$\tilde{\sigma} \equiv \frac{V_\Omega}{U_{\rm M}} \sigma, \tag{2}$$

$$\langle \sigma \rangle \equiv \frac{\int \sigma {\rm d}V}{V_\Omega}, \tag{3}$$

where V_Ω is the volume of Ω. Using the above normalized stress, the virial theorem (1) is reduced to the simple form

$$\sum_i \langle \tilde{\sigma}_i \rangle = 1. \tag{4}$$

Following Eq. (4) under the axisymmetric configuration, we obtained the poloidal rotation number $N = I_\phi / I_\theta$ of helical coils, where I_ϕ and I_θ are toroidal and poloidal currents respectively, which satisfy the uniform stress condition $\langle \sigma_\theta \rangle = \langle \sigma_\phi \rangle$ and named the coil as a virial-limit coil (VLC), whereas conventional FBC reduces stress $\langle \sigma_\phi \rangle = 0$ in the toroidal direction only [9], [10]. According to Fig. 3 in Ref [10], VLC with circular cross section of aspect ratio $A = R/a = 2$, where R and a are major and minor radii respectively, can produce 1.4 times stronger magnetic field and reduces maximum stress to about half compared with that of TF coils,

III. Design of a VLC tokamak

Since actual helical coils do not satisfy the axisymmetric assumption, we have numerically investigated the distribution of stress in a cable-in-conduit (CIC) cable by use of "NASTRAN" which is a numerical structural analysis code

TABLE I

MAXIMUM VALUE $\sigma_{\mathrm{v}_{\max}}$ AND MINIMUM VALUE $\sigma_{\mathrm{v}_{\min}}$ OF VON MISES STRESS WITH $R = 0.30$ M, $a = 0.14$ M, $B_\phi = 1.55$ T AT $r = R$.

stress (MPa)	VLC (pitch=3)	FBC (pitch=4)	HC (pitch=3)	HC (pitch=4)
$\sigma_{\mathrm{v}_{\max}}$	**395**	665	627	892
$\sigma_{\mathrm{v}_{\min}}$	66.4	164	**49.2**	127
$\lvert\sigma_{\mathrm{v}_{\max}} - \sigma_{\mathrm{v}_{\min}}\rvert$	**329**	501	578	765

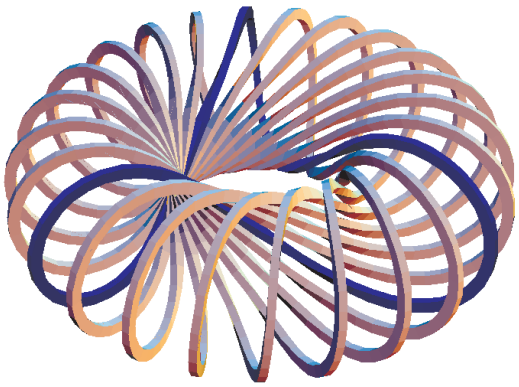

Fig. 1. VLC winding of Todoroki-II.

by a finite element method (FEM). Von Mises stress σ_{v} is an index for breaking strength of materials based on a distortional energy theory. The results of computations are listed in Table I, where HC means a simple helical coil whose orbit is $\theta = N\phi$ without pitch modulations to reduce vertical field and tilting force. This table also shows that VLC has the minimum stress and achieves a flattened distribution of stress.

The other important problem of FBC tokamak was stray magnetic field due to the helical winding. Since strong vertical fields were generated in the previous FBC tokamak Todoroki-I, an auxiliary coil set to cancel the vertical fields and an electrode for successive ionization were required for plasma discharge. To minimize the stray vertical fields, we have modulated the helical winding in such a way that the poloidal field exists only out of the torus [3]. The modulation reduces the level of the stray poloidal field B_{p}/B_ϕ in a VLC tokamak to less than 10^{-3} which is 1/10 of that in Todoroki-I. This modulation also makes the winding directions to be nearly vertical and horizontal in the outer and the inner sides of torus, respectively, as shown in Fig. 1.

Using the above analysis, we designed and manufactured a small VLC tokamak "Todoroki-II" whose parameters are listed in Table II where the achieved values of Todoroki-I are also presented. The virial-limit winding of Todoroki-II is illustrated in Fig. 1, in which a VLC is shown by darker hatch. This winding is convenient to make room for ports.

IV. OPERATION OF A VLC TOKAMAK

In a usual tokamak, CS is used to initiate and ramp up the plasma current under nearly constant toroidal magnetic field, while a VLC tokamak cannot keep the toroidal field in the ramp-up phase since VLC is a hybrid coil of CS and

TABLE II

SIZE AND OPERATIONAL PARAMETERS.

Parameters	Todoroki-I(FBC)	Todoroki-II(VLC)
Major radius	0.297 m	0.300 m
Minor radius of FBC/VLC	0.115 m	0.140 m
Winding pitch of FBC/VLC	5	3
Pole number of FBC/VLC	8	8
Plasma minor radius	0.055 m	0.070 m
Maximum toroidal field at axis	0.90 T	1.55 T
Maximum plasma current	10 kA	40 kA
Stray field level B_z/B_ϕ	1×10^{-2}	1×10^{-3}

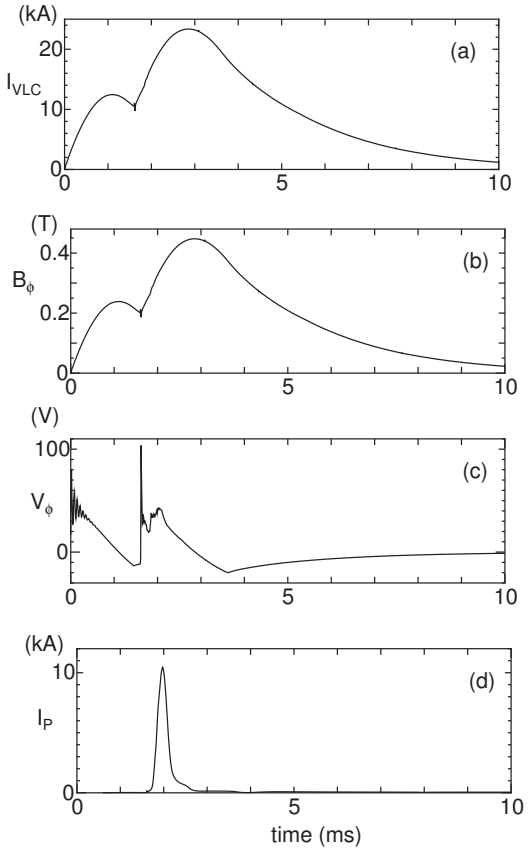

Fig. 2. Time evolutions of VLC current (a), toroidal field (b), loop voltage (c), plasma current (d) of a two-step discharge in Todoroki-II.

TF coils. In the tokamak operation with the hybrid coil, the rise of the toroidal field synchronizes with the ramp up of the plasma current. Because plasma initiation requires toroidal field, the VLC tokamak uses a two-step discharge [5], which was demonstrated in Todoroki-I. In the two-step discharge, toroidal field is created in the first ramp, and the loop voltage is utilized in the second ramp.

The first plasma discharge in Todoroki-II is shown in Fig. 2 where a two-step discharge was also demonstrated. Although the loop voltage V_ϕ was about 50 V and was expected to be large enough to initiate plasma in a stray field level of $B_z/B_\phi \sim 10^{-3}$, pre-ionization was needed while electron supply by electrode discharge during plasma discharge was not required. Next, we apply vertical fields by vertical field coils (VFCs) in order to improve the plasma discharge since plasma

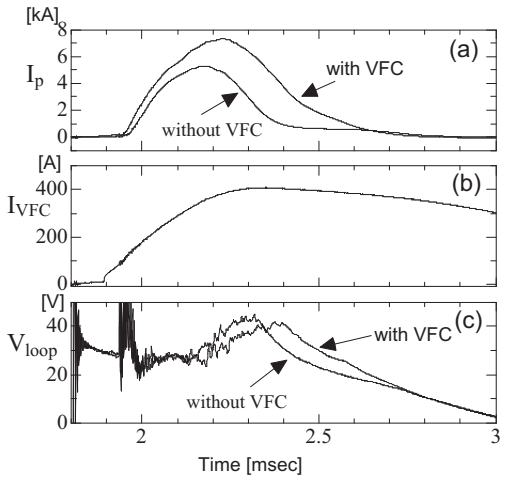

Fig. 3. Plasma discharges with/without vertical field coils. Time evolutions of plasma current (a), vertical filed coil current (b), loop voltage (c) are depicted.

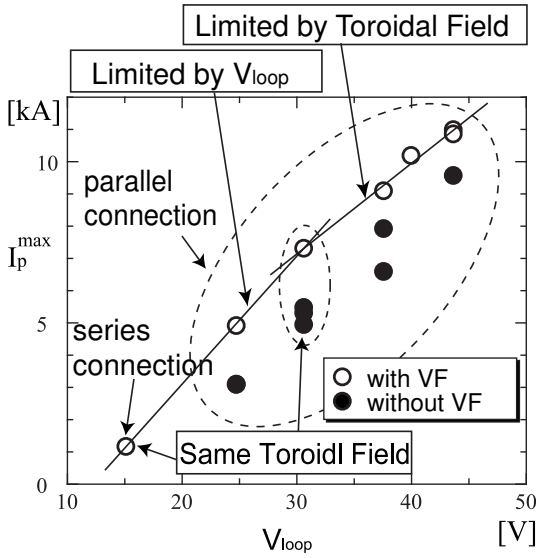

Fig. 4. Relations of maximum of plasma current and loop voltages in experiments. White and black circles show the case with/without vertical field, respectively.

equilibrium without VFC is sustained only by vertical field of eddy current. An improvement of discharge was achieved as shown in Fig. 3. External vertical field increased both the plasma pulse length and current to 1 ms and 11 kA, respectively.

Since Todoroki-II has two set of VLCs, both a series connection and a parallel connection with a power supply are available. The series connection elongates an operation time of the power supply, while it reduces the loop voltage. Relations of the maximum plasma current in several discharges and applied loop voltages are depicted in Fig. 4. When the loop voltage is less than 30 V, plasma current linearly increases with the loop voltage. In this region, plasma current is limited by the loop voltage. When the loop voltage is more than 30 V, plasma current also increases with the loop voltage while its increase-rate is reduced compared with the cases of $V_{\rm loop} < 30$ V. Since toroidal field synchronizes with plasma current in the VLC tokamak, safety factor on the plasma surface is reduced by the fast current ramp-up with a large loop voltage. In the cases of $V_{\rm loop} > 30$ V, plasma current is limited by the surface safety factor $q > 3$.

V. Plasma Shape Reproduction by Cauchy-condition surface method [8]

A shape reproduction problem can be categorized as a kind of inverse problem for Maxwell's equations. A tokamak plasma, of which the typical case is shown in Fig. 5, is generally surrounded by magnetic sensors that are located along the closed line on the poloidal cross-section. In this work, 8 flux loops and 10 magnetic probes are located in the vacuum vessel. Poloidal field coils are located in the outer region surrounding the closed line of sensor locations. Eddy currents may be induced in the vacuum vessel conductors during a transient period such as breakdown and plasma-current ramp up. Although it is possible to account for eddy current effects in a similar way to other methods, we neglect the effect in this work for simplicity.

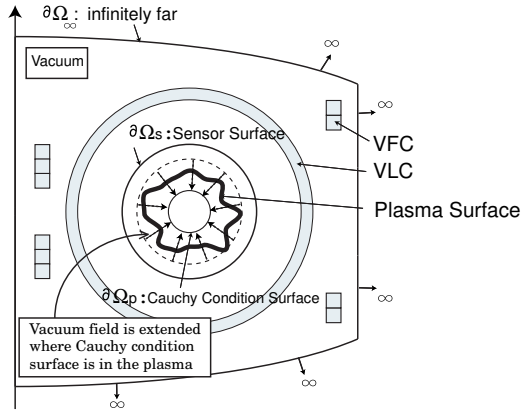

Fig. 5. Topological concept of axisymmetric tokamak geometry for plasma shape reproduction problem.

The static Maxwell's equation, $\nabla \times \boldsymbol{B} = \mu_0 \boldsymbol{j}$, in a toroidal axisymmetric region analytically yields the following integral relation by the introduction of Green's function:

$$\begin{aligned} c\psi(\boldsymbol{x}) &+ \int_{\partial\Omega} [G(\boldsymbol{x},\boldsymbol{x}')\nabla\psi(\boldsymbol{x}') \\ &- \psi(\boldsymbol{x}')\nabla G(\boldsymbol{x},\boldsymbol{x}')] \cdot \frac{\mathbf{d}\boldsymbol{l}}{r'^2} \\ &= \int_\Omega G(\boldsymbol{x},\boldsymbol{x}')\mu_0 j_\phi(\boldsymbol{x}')\frac{\mathbf{d}\boldsymbol{S}}{r'} \end{aligned} \tag{5}$$

where ψ is the poloidal flux function, G is Green's function (a response function for toroidal current in axisymmetric geometry) defined by the following equation;

$$\begin{aligned} G(\boldsymbol{x},\boldsymbol{x}') &= \mu_0\sqrt{rr'}\left\{\left(\frac{2}{k}-k\right)K(k) - \frac{2}{k}E(k)\right\} \quad (6) \\ k^2 &= \frac{4rr'}{(r+r')^2+(z-z')^2}, \\ \boldsymbol{x} &= (r,z), \end{aligned}$$

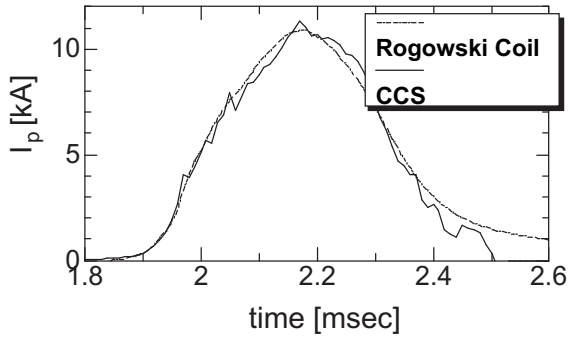

Fig. 6. Time evolutions of plasma current. A solid and dashed lines are evaluated by CCS method and rogowski coil, respectively.

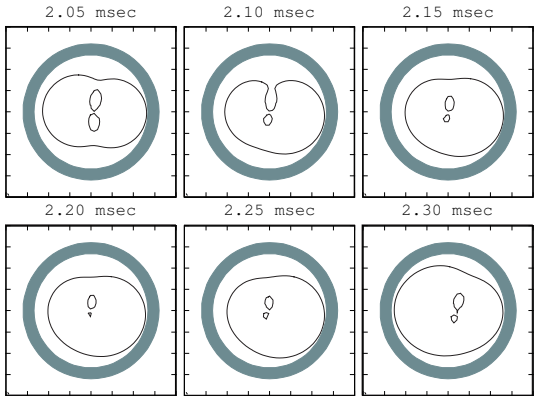

Fig. 7. A time evolution of the outer-most flux surface of plasma.

where K and E are the complete elliptic integrals of the first and second kinds, Ω is the entire region containing the known current sources (e.g. poloidal field coils), $\partial\Omega$ is the boundary surface of Ω, j_ϕ is the current density, and c is a constant (8π for $\boldsymbol{x}$ in the Ω interior, 4π for $\boldsymbol{x}$ on $\partial\Omega$, 0 for $\boldsymbol{x}$ in the Ω exterior). The ways to choose the integral region Ω and the observation point $\boldsymbol{x}$ generate different sets of equations. Here we define a surface $\partial\Omega_{\rm p}$ enclosing the entire plasma region. Now the outer region bounded by $\partial\Omega_{\rm p}$ is defined as the analyzed region $\Omega_{\rm p}$. In the region $\Omega_{\rm p}$ interior, the right-hand side of Eq. (5) is entirely provided by coil current measurements in the power supply system with eddy currents in the vacuum vessel or other conductors. The second term of the left-hand side is provided by plasma current, and the integral along the boundary surface $\partial\Omega_{\rm p}$, in which the distributed variables of the Cauchy condition (both Dirichlet and Neumann conditions) are involved as unknown quantities. Consequently, if this Cauchy condition is determined from the sensor signals, the analytical solution (Eq. (5)) must realize the precise shape reproduction, of which accuracy corresponds to that of the obtained Cauchy condition.

In this work, we apply the Cauchy-condition surface (CCS) method to VLC tokamak Todoroki-II. Although axisymmetric geometry is assumed in the CCS method, VLC is not axisymmetric. Then VLCs are simulated by 359 poloidal field coils in this work. CCS method can also evaluate plasma current. In ramp-up phases, large eddy current is induced and may degrade CCS accuracy. However, net toroidal eddy current is zero, because the vacuum vessel of Todoroki-II are composed of three insulated blocks. In Fig. 6, plasma currents evaluated from rogowski coils and CCS method are compared. A good agreement of the two methods are obtained, and the validity of CCS is proved. Finally we estimate the outer most flux surface of plasma by CCS method. Although discharge time is short and eddy current is not negligible, plasma position and surface are obtained as shown in Fig. 7.

VI. Summary and Discussions

Using the virial theorem, we have manufactured a small VLC tokamak "Todoroki-II", and its plasma discharge has started. As has been shown in this work, the problems in Todoroki-I are solved in Todoroki-II. Plasma production without continuous electrode discharge was demonstrated. Plasma discharge and control by additional vertical field was also demonstrated, and plasma current of 11 kA, which exceeded that of Todoroki-I, was achieved. Moreover, plasma current and surface are evaluated by the CCS method, and validity of CCS method for a small pulsed tokamak was verified.

Although the cross section of Todoroki-II is a circle owing to restrictions of budget, high elongation and low aspect ratio make directions of VLC winding become more vertical and horizontal, which configuration is similar to that of CS and TF coil system in a conventional tokamak. Therefore, a VLC tokamak reactor can utilize blanket and the other parts in a conventional tokamak reactor with much reduced volume of coils and their supporting structure.

Acknowledgment

The authors would like to thank Dr. K. Kurihara (JAERI) for many useful discussions and comments. This work was supported in part by New Energy and Industrial Technology Development Organization, Japan.

References

[1] S. Tsuji-Iio, H. Tsutsui, J. Kondoh, *et al.*: Fusion Energy 1996 (Proc. 16th IAEA Fusion Energy Conf., Montreal, 1996), Vol. 3, IAEA, Vienna (1997) 685-692.
[2] Y. Miura, J. Kondoh, R. Shimada: in Fusion Technology (Proc. 18th Eur. Symp. Karlsruhe, 1994), Vol. 2, Elsevier, Amsterdam (1995) 957-960.
[3] J. Kondoh, T. Fujita, H. Tsutsui *et. al.*: T.IEE Japan, **118-B**, No.2, (1998) 191-198 (in Japanese).
[4] T. Murakami *et. al.*: Fusion Engineering and Design, **51-52** (2000) 1059-1064.
[5] S. Tsuji-Iio *et. al.*: Fusion Energy 1998 (2001 Edition) (Proc. 17th IAEA Fusion Energy Conf. Yokohama, 1998) IAEA, Vienna (2001) FTP-30.
[6] T. Murakami *et. al.*: J. Plasma Fusion Research, **75**, No.3, 1999, pp.264-274 (in Japanese).
[7] S. Yoshikawa: Phys. Fluid, **7**, 1963, pp.278.
[8] K. Kurihara: Fusion Eng. Des., **51-52**, 2000, pp.1049-1057.
[9] H. Tsutsui, S. Nomura, R. Shimada: J. Plasma and Fusion Research, **77**, No.3, 2001, pp.300-308 (in Japanese).
[10] H. Tsutsui, K, Nakayama, S. Nomura, R. Shimada, S. Tsuji-Iio: IEEE Trans. Appl. Supercond., **12**, No.1, 2002, pp.644-647.